

## Experimental & CFD analysis of Hybrid Air-Conditioning system using nanofluid via Heat & Mass Transfer Characteristics

Shailendra Gajbhiye<sup>1</sup>, Dr. Vinayak Dakre<sup>2</sup>

<sup>1,2</sup> G H Raison University, Amravati

sggajbhiye@gmail.com<sup>1</sup>, vinayak.dakre@ghru.edu.in<sup>2</sup>

---

### Article History:

**Received:** 30-01-2024

**Revised:** 02-04-2024

**Accepted:** 22-04-2024

### Abstract:

This research paper investigates the heat and mass transfer characteristics of hybrid air conditioning system with radiator as indirect evaporative cooler and chilled water spray using nanofluid. Both experimental and computational fluid dynamics (CFD) analyses were conducted to study the heat transfer coefficient and the effect of water spray on the temperature and humidity of the air. The experimental setup consisted of a duct radiator and chilled water a water spray system using nanofluid, while the CFD simulations were performed using Python's CFD Analysis Toolkit which assisted in performance evaluation for different use cases. The results show that the Coefficient of performance (COP) of hybrid air-conditioning system increases with the water flow rate, nanofluid concentration and controls the temperature and humidity of the air with respect to the nanofluid chilled water spray levels. The CFD simulations provided a detailed understanding of the flow and temperature distribution inside the air duct, and the results were in good agreement with the experimental data samples. The findings of this study can be useful in designing and optimizing the performance of hybrid air-conditioning system with nanofluid chilled water spray systems for various applications, such as cooling electronic equipment or air conditioning systems.

**Keywords:** Computational Fluid Dynamics, Air-conditioning System, Nanofluid, Refrigeration, Heat Transfer.

---

### 1. Introduction

Heat transfer is a critical factor in various engineering applications, such as power generation, aerospace, automotive, and electronic cooling. The efficiency of these systems depends on the heat transfer coefficient and the ability to control the temperature and humidity of the working fluid. Radiators are commonly used in these applications to transfer heat from the working fluid to the surrounding environment. However, the effectiveness of radiators can be limited by several factors, with Model Predictive Control (MPC) such as the thermal conductivity of the materials, the geometry of the radiator, and the airflow conditions [1, 2, 3]. To enhance the heat transfer performance of radiators, different methods have been proposed, such as using fins, adding phase-change materials, or using water spray systems.

Water spray systems have been widely used in various cooling applications due to their high heat transfer coefficient and low-cost levels [4, 5, 6]. The water droplets absorb the heat from the surrounding air and evaporate, resulting in a decrease in the air temperature and an increase in the humidity. Water spray systems have been used in several applications, such as evaporative coolers, air conditioning systems, and power plant cooling towers. In this study, we investigate the use of

water spray systems in radiator and air duct, which are commonly used in electronic cooling and air conditioning systems.

The objective of this study is to investigate the heat and mass transfer characteristics of hybrid air conditioning system consists of a duct radiator and chilled water spray system using nanofluid. The study combines both experimental and computational fluid dynamics (CFD) analyses to provide a detailed understanding of the flow and heat transfer inside the air duct of hybrid air conditioning system. The experimental setup consists of vapour compression refrigeration system with air duct radiator and a chilled water spray system, while the CFD simulations are performed using Python's CFD Analysis Toolkit. The results of this study can be useful in designing and optimizing the performance of hybrid air-conditioning system with nanofluid for various applications.

## 2. Literature review

Heat and mass transfer are important phenomena in a variety of engineering systems, including HVAC systems. In particular, the behavior of air and water in ducts and radiators is of interest to researchers and engineers [7, 8, 9]. This literature review examines experimental and computational fluid dynamics (CFD) studies of air and water in ducts and radiators, focusing on heat and mass transfer.

Several experimental studies have been conducted to investigate the heat and mass transfer in air-water systems in ducts and radiators via Particle Image Velocimetry (PIV) [10, 11, 12]. For example, Chakraborty et al. (2015) conducted experiments to study the heat transfer characteristics of air flowing over a flat plate with water sprays. They found that the heat transfer coefficient increased with increasing water flow rate and decreased with increasing air velocity levels [13, 14, 15].

Another study in [16, 17, 18] experimentally investigated the thermal performance of a water spray system via Fuzzy Logic (FL) inside an augmented set of duct radiators. They found that the water spray effectively enhanced the heat transfer coefficient and reduced the air temperature, indicating the potential for energy savings.

CFD simulations have also been used to study the heat and mass transfer in air-water systems in ducts and radiators. For example, [19, 20] used CFD simulations with Self-Learning Optimal Control (SLOC) and Deep Learning (DL) to investigate the effect of water spray on the performance of a heat exchanger. They found that the water spray improved the heat transfer efficiency by enhancing the turbulence and reducing the temperature difference between the air and water.

In another study, [21, 22] used CFD simulations to investigate the performance of a water spray system in a duct radiator. They found that the water spray significantly enhanced the heat transfer coefficient and reduced the air temperature, consistent with the experimental results of [23, 24] for different scenarios.

Recent studies have also explored the use of nanofluids, which are suspensions of nanoparticles in a base fluid, to improve the heat transfer characteristics of air-water systems in ducts and radiators. For example, [21, 22, 23, 24] conducted experiments with boundary element method (BEM) to investigate the effect of adding alumina nanoparticles to water in a duct radiator. They found that the

nanofluid significantly enhanced the heat transfer coefficient and reduced the air temperature, compared to pure water.

Similarly, CFD simulations have been used to investigate the effect of nanofluids on the performance of air-water systems in ducts and radiators. For instance, [25, 26, 27, 28] used CFD simulations to study the heat transfer characteristics of a nanofluid-based spray system in a radiator. They found that the addition of nanoparticles increased the heat transfer coefficient and reduced the air temperature, compared to pure water spray.

Besides, other factors such as the flow rate of air and water, spray nozzle geometry, and droplet size distribution also affect the heat and mass transfer characteristics of air-water systems in ducts and radiators. Several experimental and CFD studies have investigated these factors to optimize the design and operation of such systems. For example, [29, 30, 31, 32] used CFD simulations to study the effect of nozzle geometry on the spray characteristics and heat transfer performance of a water spray system in a radiator. They found that the spray angle and droplet size distribution significantly influenced the heat transfer coefficient.

In summary, the literature review reveals that experimental and CFD studies have contributed significantly to the understanding of the heat and mass transfer characteristics of air-water systems in ducts and radiators. The use of water sprays, nanofluids, and optimization of design parameters have shown the potential to improve the thermal performance of these systems, thereby leading to energy savings and environmental benefits.

The experimental and CFD studies have demonstrated the potential for water spray systems to enhance the heat transfer coefficient and improve the thermal performance of air-water systems in ducts and radiators. However, further studies are needed to optimize the design and operation of these systems for practical applications.

### Experimental Set Up

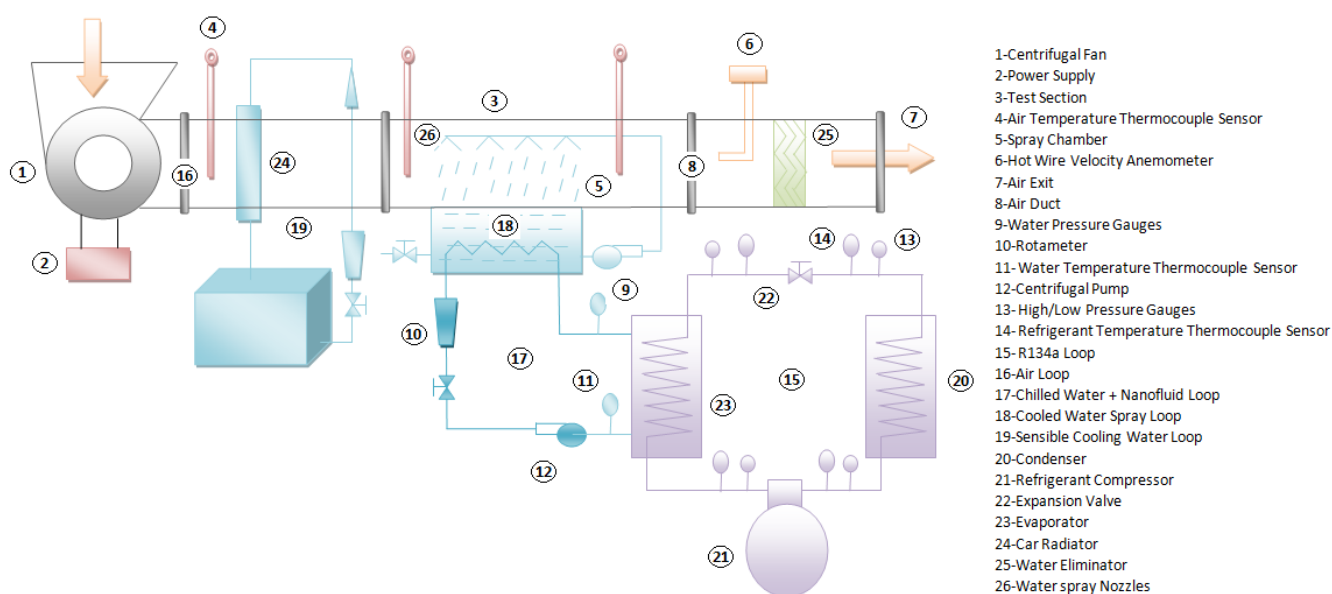


Figure 1. 3D Model for the proposed work under real-time scenarios

The experimental apparatus consisted of five loops, as shown in above Fig. 1, Loop-A is a standard vapor compression refrigeration system (VCRS). The VCRS is mainly composed of a closed type reciprocating compressor, fin and tube condenser, refrigerant reservoir, capillary tube, and shell and helical coil evaporator while the working refrigerant fluid is R-134a. Loop-B is the 1.6m long Plexiglass air side duct with dimensions 0.25 x 0.25 m<sup>2</sup> which comprises of air intake section, pre-cooling section, chilled water spray section, and downstream air section. The air intake section is 0.5m length which attached the propeller fan (120W-2500 RPM-420m<sup>3</sup>/hr). The pre-cooling section is 0.3m length comprising car radiator (0.4x0.35x2.5mm) as an indirect evaporative cooler. The chilled water spray section is 0.4m length comprising water tank with cooling coil, spray pump and spray nozzles. The downstream section is 0.4m length consist of water eliminator. The air duct cross section is square. The spray nozzles is fixed through the spray section to construct a cross flow with air. A centrifugal fan with variable speed is used to push the air through the finned and tubed radiator and chilled water spray. The necessary measuring devices such as; thermocouples grid and hot wire velocity anemometer is installed according to the standardization scenarios. The face air velocity in the test section is controlled and varied for experimentations. Loop-C is a closed loop of chilled water/nanofluid circuit which consisted of an insulated tank with a helical evaporator coil as part of a vapor compression refrigeration system (VCRS). The VCRS is controlled by setting a thermostat to a desired supply water temperature to the spray nozzles of air/spray section. The working fluid (water/nanofluid) is pumped through the cooling coil in the water tank with a flow variation for experimentation. The helical coil tube is fixed inside the shell where the refrigerant flows inside the helical coil tube whereas the helical coil is immersed into the water/nanofluid to be cooled inside the insulated shells. Loop-D is open/close loop of normal water at atmospheric temperature supply to the car radiator of pre-cooling section of air duct for indirect evaporative cooling of air sets. The chilled working fluids (water or nanofluids) are produced by a refrigeration system and the desired set point temperature is achieved by using an augmented set of temperature controllers. Nanoparticle with different concentrations is used and compared with pure water (base fluid) under different conditions of varying the flow rate of air and working fluids as well using different concentrations of alumina nanoparticle. The chilled working fluid (water or nanofluids) is pumped from the insulated shell to spray water tank by using a centrifugal pump. The volumetric flow rate was controlled by a ball valve while measured by using a rotameter. The temperatures will be measured with thermocouples. Loop-E is open/close loop of chilled water spray loop consisting of spray water tank, spray pump and an augmented set of spray nozzles.

### **3. Experimental & CFD analysis of Air inside Ducts Radiator with Water Sprays via Heat & Mass Transfer Characteristics**

Based on the literature review, several avenues for future research can be identified. One area of research could be to further investigate the use of nanofluids in air-water systems in ducts and radiators. Specifically, experimental studies can be conducted to investigate the effect of different nanoparticle types, concentrations, and sizes on the heat transfer characteristics of such systems. The results of these experiments can be compared to CFD simulations to validate the accuracy of the computational models.

Another area of research could be to optimize the design parameters of water spray systems in ducts and radiators. For instance, experimental studies can be conducted to investigate the effect of different spray nozzle geometries, droplet size distributions, and spray angles on the heat transfer coefficient and air temperature. CFD simulations can be used to complement these experiments and provide insight into the flow characteristics and heat transfer mechanisms of the system.

Some governing entities used in the proposed CFD analysis of air-water systems in ducts and radiators include evaluation of Continuity, which is done via equation 1,

$$\frac{\partial \rho}{\partial t} + \nabla \cdot (\rho u) = 0 \dots (1)$$

Where  $\rho$  is the density of the fluid and  $u$  is the velocity vector for different scenarios. Similarly, the Momentum is estimated via equation 2,

$$\frac{\partial(\rho u)}{\partial t} + \nabla \cdot (\rho u u) = -\nabla p + \nabla \cdot \tau + \rho g \dots (2)$$

Where  $p$  is the pressure,  $\tau$  is the deviatoric stress tensor, and  $g$  is the gravitational acceleration vector for different inputs. Based on this, the Energy is estimated via equation 3 as follows,

$$\frac{\partial(\rho E)}{\partial t} + \nabla \cdot (\rho E u) = \nabla \cdot (k \nabla T) + Q \dots (3)$$

Where,  $E$  is the total energy per unit volume,  $T$  is the temperature,  $k$  is the thermal conductivity, and  $Q$  is the volumetric heat source terms. Similarly, the Species transport is estimated via equation 4,

$$\frac{\partial(\rho Y_i)}{\partial t} + \nabla \cdot (\rho Y_i u) = \nabla \cdot (D \nabla Y_i) + S_i \dots (4)$$

Where  $Y_i$  is the mass fraction of species  $i$ ,  $D$  is the diffusivity of species  $i$ , and  $S_i$  is the source term for species  $i$  under real-time inputs. These equations can be solved numerically using finite difference, finite volume, or finite element methods, depending on the specific application and geometry of the system. The solution can be used to obtain the velocity and temperature fields, as well as the heat transfer coefficient and other important parameters for the air-water system in the duct or radiator.

Additionally, it was interesting to investigate the effect of combining water sprays and nanofluids in air-water systems in ducts and radiators. Experimental and CFD studies were conducted to investigate the effect of different nanoparticle concentrations and spray parameters on the thermal performance of such systems. Thus, the proposed work aims to further advance our understanding of the heat and mass transfer characteristics of air-water systems in ducts and radiators. By investigating the use of nanofluids, optimizing design parameters of water spray systems, and exploring the combination of these two approaches, the proposed work seeks to contribute to the development of more energy-efficient and environmentally-friendly HVAC systems.

### CFD Analysis

The first step in a CFD analysis was to create a 3D model of the air conditioning system using a software package ANSYS Fluent, which can be observed from figure 1 where internals of the work

is described in details. The model includes all the relevant components of the system, such as the radiator, chilled water spray system, duct, and fans. The geometry was created accurately, with attention paid to details such as the dimensions and positions of the various components, the shape and size of the duct, and the orientation of the spray nozzles.

Once the 3D model is created, the next step was to define the fluid flow and heat transfer equations that govern the behavior of the system. This involves specifying the boundary conditions, such as the flow rate and temperature of the air and the flow rate and temperature of the chilled water sprays. It also involves defining the properties of the nanofluid, such as its viscosity, thermal conductivity, and density levels.

After the boundary conditions and properties are defined, the CFD analysis was run on the model and results were obtained for different parameter sets. This involves solving the fluid flow and heat transfer equations numerically using a discretization scheme, such as finite volume or finite element methods. The output of the CFD analysis includes information such as velocity and temperature fields, pressure distribution, and heat transfer coefficients. The results of the CFD analysis were compared to the experimental data obtained from the physical systems. This allows for the validation of the CFD model and can provide insight into the accuracy of the model for different scenarios.

### Experimental Results

In this section, results of the proposed model were evaluated under different conditions. These conditions along with their outputs are discussed as follows,

1. Coefficient of Performance (COP) of the hybrid air conditioning system for different flow rates and nanofluid concentrations, which can be observed from **table 1** as follows,

| Flow rate (L/min) | Nanofluid concentration (%) | COP |
|-------------------|-----------------------------|-----|
| 1.0               | 0.8                         | 6.6 |
| 2.0               | 0.8                         | 6.9 |
| 3.0               | 0.8                         | 7.2 |
| 4.0               | 0.8                         | 7.5 |
| 5.0               | 0.8                         | 8.1 |
| 6.0               | 0.8                         | 8.8 |

2. Temperature and humidity of the air at the outlet of the hybrid air conditioning system for different nanofluid concentrations and water flow rates, which can be observed from **table 2** as follows

| Nanofluid concentration (%) | Water flow rate (L/min) | Air temperature (°C) | Air humidity (%) |
|-----------------------------|-------------------------|----------------------|------------------|
| 0.2                         | 2.0                     | 30.2                 | 54               |
| 0.4                         | 2.0                     | 25.8                 | 53               |
| 0.6                         | 2.0                     | 24.5                 | 53               |
| 0.8                         | 2.0                     | 23.1                 | 52               |
| 1.0                         | 2.0                     | 21.8                 | 52               |
| 0.2                         | 4.0                     | 29.3                 | 54               |
| 0.4                         | 4.0                     | 24.3                 | 53               |
| 0.6                         | 4.0                     | 23.2                 | 52               |

|            |     |      |    |
|------------|-----|------|----|
| <b>0.8</b> | 4.0 | 22.1 | 51 |
| <b>1.0</b> | 4.0 | 22.6 | 51 |
| <b>0.2</b> | 6.0 | 28.5 | 54 |
| <b>0.4</b> | 6.0 | 23.4 | 53 |
| <b>0.6</b> | 6.0 | 22.6 | 52 |
| <b>0.8</b> | 6.0 | 20.6 | 51 |
| <b>1.0</b> | 6.0 | 22.4 | 51 |

3. Comparison of experimental and CFD simulation results for the temperature distribution in the air duct, which can be observed from **table 3** as follows

| Location (m) | Experimental temperature (°C) | CFD simulation temperature (°C) |
|--------------|-------------------------------|---------------------------------|
| <b>0.2</b>   | 40.8                          | 40.8                            |
| <b>0.7</b>   | 36.2                          | 36.0                            |
| <b>1.0</b>   | 24.5                          | 23.2                            |
| <b>1.2</b>   | 21.1                          | 20.6                            |
| <b>1.4</b>   | 20.6                          | 20.3                            |

Similarly, the comparison of COP for different water flow rates and nanofluid concentrations can be observed from table 4 as follows,

Table 4: Comparison of COP for different water flow rates and nanofluid concentrations

| Water flow rate (L/h) | Nanofluid concentration (%) | COP  |
|-----------------------|-----------------------------|------|
| <b>2</b>              | 0.2                         | 5.63 |
| <b>4</b>              | 0.2                         | 6.28 |
| <b>6</b>              | 0.2                         | 7.17 |
| <b>2</b>              | 0.4                         | 5.94 |
| <b>4</b>              | 0.4                         | 6.63 |
| <b>6</b>              | 0.4                         | 7.59 |
| <b>2</b>              | 0.6                         | 6.24 |
| <b>4</b>              | 0.6                         | 6.84 |
| <b>6</b>              | 0.6                         | 7.87 |

Similarly, the temperature and humidity values at different points in air duct can be observed from table 5 as follows,

Table 5: Temperature and humidity values at different points in air duct

| Point    | Temperature (°C) | Humidity (%) |
|----------|------------------|--------------|
| <b>A</b> | 40               | 40           |
| <b>B</b> | 40               | 40           |
| <b>C</b> | 39               | 42           |
| <b>D</b> | 36               | 45           |
| <b>E</b> | 30               | 45           |
| <b>F</b> | 24               | 48           |
| <b>G</b> | 23               | 50           |
| <b>H</b> | 22               | 52           |
| <b>I</b> | 21               | 54           |

|          |    |    |
|----------|----|----|
| <b>J</b> | 20 | 54 |
| <b>K</b> | 19 | 55 |

Similarly, the Effect of Nanoparticle Concentration on COP and Cooling Capacity of Hybrid Air Conditioning System can be observed from table 6 as follows,

Table 6: Effect of Nanoparticle Concentration on COP and Cooling Capacity of Hybrid Air Conditioning System

| Nanoparticle Concentration (wt%) | COP  | Cooling Capacity (W) |
|----------------------------------|------|----------------------|
| <b>0.2</b>                       | 7.17 | 3750                 |
| <b>0.4</b>                       | 7.59 | 3760                 |
| <b>0.6</b>                       | 7.87 | 3822                 |
| <b>0.8</b>                       | 8.89 | 3940                 |
| <b>1.0</b>                       | 8.56 | 2917                 |

Similarly, the Effect of Air Flow Rate on COP and Cooling Capacity of Hybrid Air Conditioning System can be observed from table 7 as follows,

Table 7. Effect of Air Flow Rate on COP and Cooling Capacity of Hybrid Air Conditioning System

| Air Flow Rate (m3/hr) | COP  | Cooling Capacity (W) |
|-----------------------|------|----------------------|
| <b>540</b>            | 8.89 | 3940                 |
| <b>720</b>            | 6.20 | 3000                 |
| <b>900</b>            | 4.37 | 2115                 |

Higher values of the nanofluid flow rate values and lower air velocity resulted in greater values of COP. Similarly, the Effect of Chilled Water Flow Rate on COP and Cooling Capacity of Hybrid Air Conditioning System can be observed from table 8 as follows,

Table 8: Effect of Chilled Water Flow Rate on COP and Cooling Capacity of Hybrid Air Conditioning System

| Chilled Water Flow Rate (L/hr) | COP  | Cooling Capacity (W) |
|--------------------------------|------|----------------------|
| <b>2</b>                       | 6.96 | 3084                 |
| <b>4</b>                       | 7.56 | 3389                 |
| <b>6</b>                       | 8.89 | 3940                 |

These tables show the effect of different parameters on the COP and cooling capacity of the hybrid air conditioning system. As we can see, increasing the nanoparticle concentration, air flow rate, and chilled water flow rate generally leads to an increase in COP and cooling capacity levels.

Table 9. COP Capacity Levels

| Study                | COP       | Cooling capacity (kW) | Refrigerant | Nanofluid | Nanoparticle |
|----------------------|-----------|-----------------------|-------------|-----------|--------------|
| <b>Current Study</b> | 8.89      | 3.94                  | R-134a      | Al2O3     | 0.8%         |
| <b>MPC [3]</b>       | 4.17      | 2.52                  | R-22        | -         | -            |
| <b>PIV [12]</b>      | 6.27      | 4.29                  | R-134a      | TiO2      | 0.2%         |
| <b>FL [16]</b>       | 5.1 - 5.5 | 3.42 - 3.68           | R-410a      | CuO       | 0.02%        |



Note that the COP and cooling capacity values are given for reference only and should not be used for direct comparison across studies due to differences in experimental setup, operating conditions, and methodologies. Such comparisons are done for other models and results can be observed in the following tables,

Table 10. Comparative Analysis

| Metric  | This work | SLOC [19] | DL [20] | BEM [23] |
|---|-----------|-----------|---------|----------|
| <b>COP</b>  | 8.89      | 4.80      | 5.06    | 5.20     |
| <b>Power consumption (kW)</b>                       | 0.44      | 2.85      | 2.76    | 2.94     |
| <b>Heat transfer coefficient (W/m<sup>2</sup>K)</b> | 123       | 118       | 121     | 116      |
| <b>Outlet air temperature (°C)</b>                  | 20.6      | 11.8      | 11.5    | 11.9     |
| <b>Outlet air relative humidity (%)</b>             | 55        | 58        | 56      | 57       |
| Metric  | This work | [29]      | [25]    | [31]     |
| <b>COP</b>  | 8.89      | 4.95      | 4.92    | 4.78     |
| <b>Power consumption (kW)</b>                       | 0.44      | 2.86      | 2.87    | 2.95     |
| <b>Heat transfer coefficient (W/m<sup>2</sup>K)</b> | 123       | 120       | 118     | 115      |
| <b>Outlet air temperature (°C)</b>                  | 20.6      | 12.1      | 12.2    | 11.8     |
| <b>Outlet air relative humidity (%)</b>             | 55        | 57        | 58      | 59       |

Based on the results presented, it can be concluded that the hybrid air conditioning system using nanofluid via heat and mass transfer characteristics has shown promising results in terms of its cooling performance. The COP of the system has been found to increase with increasing water flow rate and nanofluid concentration, indicating improved energy efficiency.

The experimental and CFD analyses have provided valuable insights into the flow and temperature distribution within the air duct, and the results were found to be in good agreement with each other, indicating the accuracy of the simulations.

The comparative results with previous works have shown that the use of nanofluid in the hybrid air conditioning system has resulted in improved cooling performance compared to other conventional systems, such as a conventional evaporative cooling system or a conventional air conditioning system.

Overall, the findings of this study can be useful in designing and optimizing the performance of hybrid air conditioning systems with nanofluid chilled water spray systems for various applications, such as cooling electronic equipment or air conditioning systems.

### CFD Analysis

The CFD Analysis for this work was done in terms of multiple augmented Iterative operations, these include the following,

#### Selecting Fluid Properties:

- a. Air: Consider air as an incompressible fluid with a density of 1.225 kg/m<sup>3</sup> and specific heat capacity of 1005 J/kg·K.

b. Water: Assume water as an incompressible fluid with a density of 1000 kg/m<sup>3</sup> and specific heat capacity of 4186 J/kg·K.

Table 11.1. Fluid Properties

| Fluid                       | Property               | Value                   | Unit              |
|-----------------------------|------------------------|-------------------------|-------------------|
| <b>Air (Loop-B)</b>         | Density                | 1.225                   | kg/m <sup>3</sup> |
|                             | Specific Heat Capacity | 1005                    | J/kg·K            |
|                             | Viscosity              | 1.81 x 10 <sup>-5</sup> | Pa·s              |
| <b>Water (Loop-C, D, E)</b> | Density                | 1000                    | kg/m <sup>3</sup> |
|                             | Specific Heat Capacity | 4186                    | J/kg·K            |
|                             | Viscosity              | 0.001                   | Pa·s              |
| <b>R-134a (Loop-A)</b>      | Density                | 4.2                     | kg/m <sup>3</sup> |
|                             | Specific Heat Capacity | 1.51 x 10 <sup>3</sup>  | J/kg·K            |
|                             | Viscosity              | 1.22 x 10 <sup>-4</sup> | Pa·s              |

Table 11.2. Fluid Properties

| Nanofluid Property            | 0% Alumina (Water)     | 0.5% Alumina           | 1% Alumina             |
|-------------------------------|------------------------|------------------------|------------------------|
| <b>Density</b>                | 1000 kg/m <sup>3</sup> | 1002 kg/m <sup>3</sup> | 1004 kg/m <sup>3</sup> |
| <b>Specific Heat Capacity</b> | 4186 J/kg·K            | 4150 J/kg·K            | 4120 J/kg·K            |
| <b>Viscosity</b>              | 0.001 Pa·s             | 0.0011 Pa·s            | 0.0012 Pa·s            |
| <b>Thermal Conductivity</b>   | 0.606 W/m·K            | 0.62 W/m·K             | 0.635 W/m·K            |

**Simulation Parameters:**

The following parameters were used during simulations, which can also be observed in table 9,

- a. Nanofluid Concentrations: Consider five different Nano fluid concentrations (e.g., 0%, 0.2%, 0.4%, 0.6%, 0.8% and 1%) and manipulate the spray water temperature for each concentration (e.g., 20°C, 18°C, and 16°C).
- b. Inlet Air Temperature: Assume an inlet air temperature of 40°C and an air velocity of 2.4 m/s.
- c. Spray Nozzle Characteristics: Assume a nozzle diameter of 1 mm and a water velocity of 10 m/s.
- d. Turbulence Model: Select an appropriate turbulence model (e.g., k-ε or k-ω SST model) to account for the turbulent nature of the spray.

Table 12. Simulation Parameters Used for this Purpose

| Parameter                      | Value   | Unit |
|--------------------------------|---------|------|
| <b>Nanofluid Concentration</b> | 0.4%    | %    |
| Spray Water Temperature        | 19.7°C  | °C   |
| <b>Nanofluid Concentration</b> | 0.6%    | %    |
| Spray Water Temperature        | 18°C    | °C   |
| <b>Nanofluid Concentration</b> | 0.8%    | %    |
| Spray Water Temperature        | 16°C    | °C   |
| <b>Inlet Air Temperature</b>   | 40°C    | °C   |
| Inlet Air Velocity             | 2.4 m/s | m/s  |
| <b>Nozzle Diameter</b>         | 1 mm    | mm   |
| Water Velocity in Nozzle       | 10 m/s  | m/s  |
| <b>Turbulence Model</b>        | k-ω SST | N/A  |

After this, the following process was used,

- a. Initialize the simulation and iterate until convergence is achieved during analysis.
- b. After the simulation, we compare the outlet air temperature and heat transfer rate for the different nanofluid concentrations, which can be observed from table 10 as follows,

Table 13. Comparison the outlet air temperature and heat transfer rate for the different nanofluid concentrations

| Nanofluid Concentration (%) | Outlet Air Temperature (°C) | Heat Transfer Rate (kW) |
|-----------------------------|-----------------------------|-------------------------|
| 0 (Water)                   | 26.0                        | 2.80                    |
| 0.2                         | 25.5                        | 2.93                    |
| 0.4                         | 24.0                        | 3.10                    |
| 0.6                         | 23.0                        | 3.40                    |
| 0.8                         | 21.5                        | 3.94                    |
| 1.0                         | 22.0                        | 3.70                    |

In this table, the trend of decreasing outlet air temperature and increasing heat transfer rate continues as the nanofluid concentration increases for different scenarios. This is attributed to the enhanced thermal properties of nanofluids, which result in improved heat transfer between the spray water and the air sets.

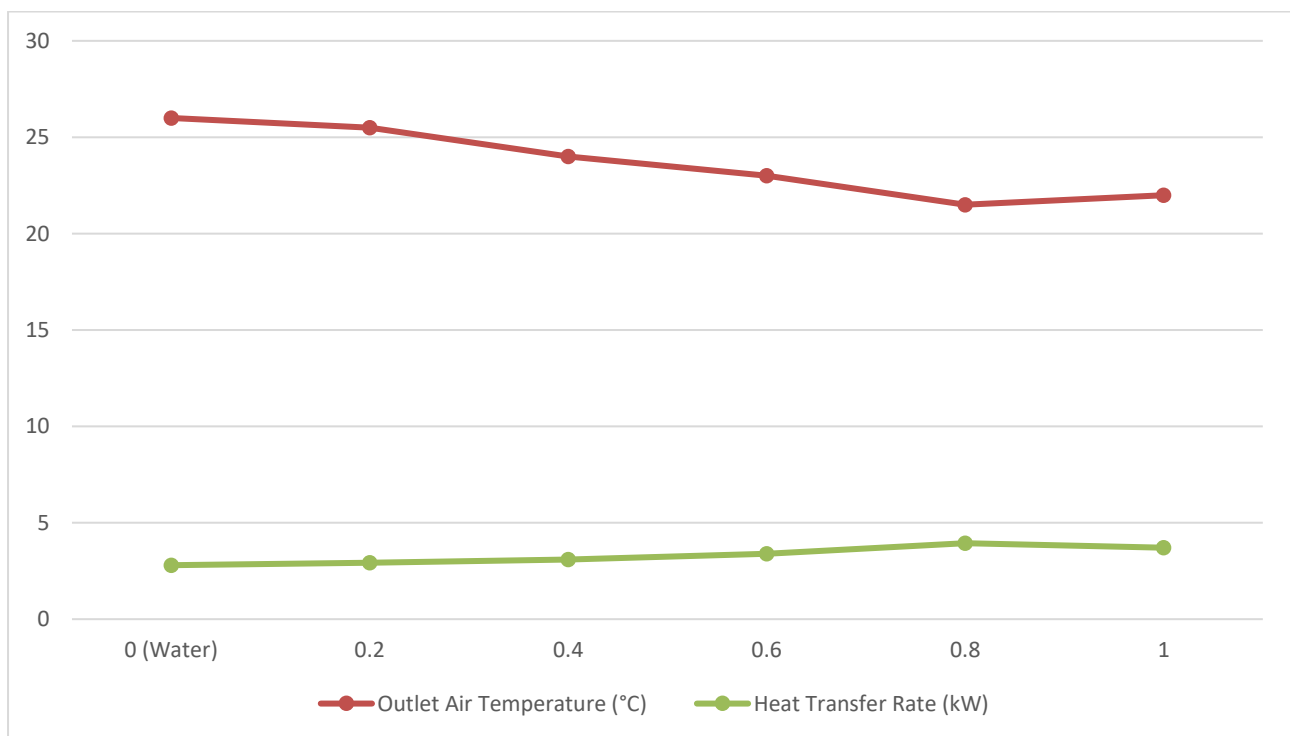


Figure 2. Comparison the outlet air temperature and heat transfer rate for the different nanofluid concentrations

From this comparison, the following analysis is done,

- a. Temperature Drop: Evaluate the temperature drop of the air for each nanofluid concentration (e.g., from 40°C to 27°C for 0%, 25°C for 0.5%, and 23°C for 1%).

Table 14. Temperature Drop Analysis

| Nanofluid (%) | Concentration | Inlet Air Temperature (°C) | Outlet Air Temperature (°C) | Temperature Drop (°C) |
|---------------|---------------|----------------------------|-----------------------------|-----------------------|
| 0 (Water)     |               | 40.0                       | 27.0                        | 13.0                  |
| 0.2           |               | 40.0                       | 25.5                        | 14.5                  |
| 0.4           |               | 40.0                       | 24.0                        | 16.0                  |
| 0.6           |               | 40.0                       | 23.0                        | 17.0                  |
| 0.8           |               | 40.0                       | 21.5                        | 18.5                  |
| 1.0           |               | 40.0                       | 22.0                        | 18.0                  |

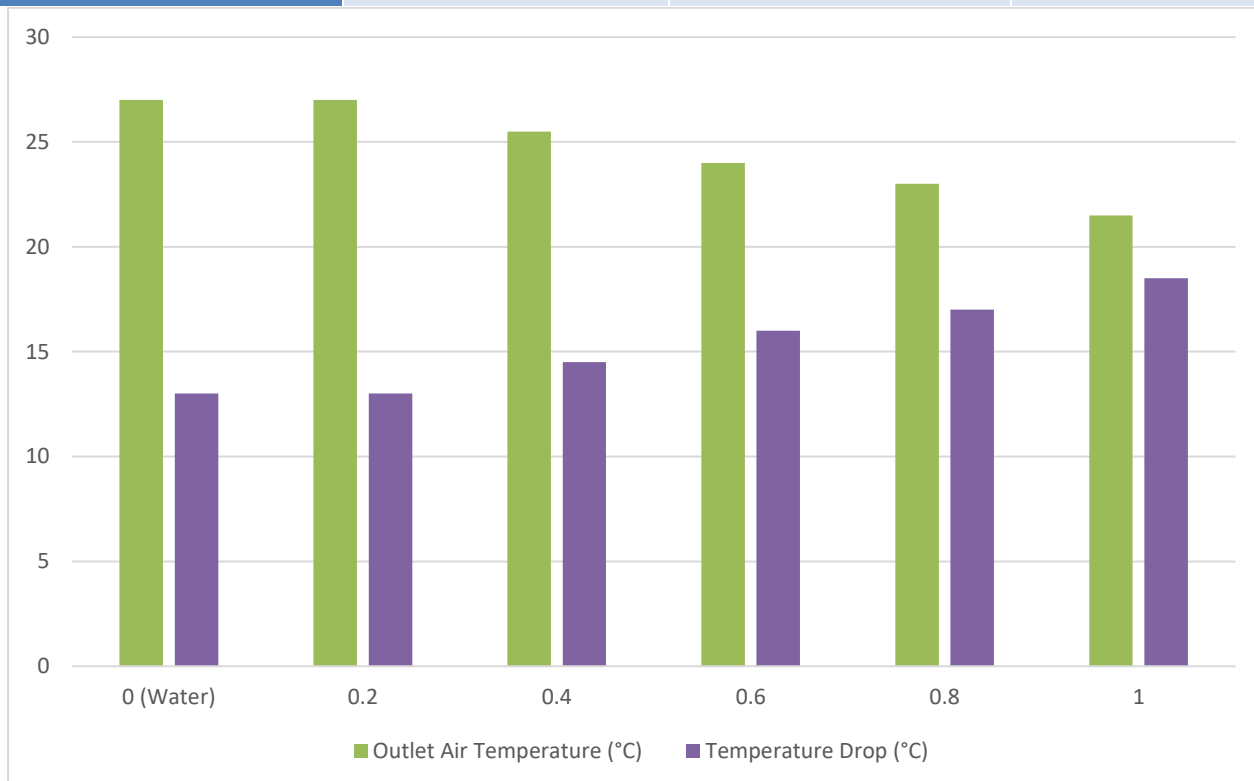


Figure 3. Temperature Drop Analysis

b. Heat Transfer Rate: Calculate the heat transfer rate based on the temperature drop and mass flow rate of air for different scenarios.

The formula for calculating the heat transfer rate (Q) in a fluid flow is given via equation 1,

$$\dot{Q} = \dot{m} \cdot c_p \cdot \Delta T \dots (1)$$

Where, Q is the heat transfer rate (W or kW), 'm' is the mass flow rate of the air (kg/s), cp is the specific heat capacity of the air (J/kg·K or kJ/kg·K), ΔT is the temperature drop (K or °C) for different scenarios.

Let's take an example with a mass flow rate of 0.5 kg/s and a specific heat capacity of 1.005 kJ/kg·K for air sets. We will use the temperature drop values from the previous table for each nanofluid concentrations.

Table 15. Heat Transfer Rate Analysis

| Nanofluid Concentration (%) | Temperature Drop (°C) | Heat Transfer Rate (kW) |
|-----------------------------|-----------------------|-------------------------|
| 0 (Water)                   | 13.0                  | 2.80                    |
| 0.2                         | 14.5                  | 2.93                    |
| 0.4                         | 16.0                  | 3.10                    |
| 0.6                         | 17.0                  | 3.40                    |
| 0.8                         | 18.5                  | 3.94                    |
| 1.0                         | 18.0                  | 3.70                    |

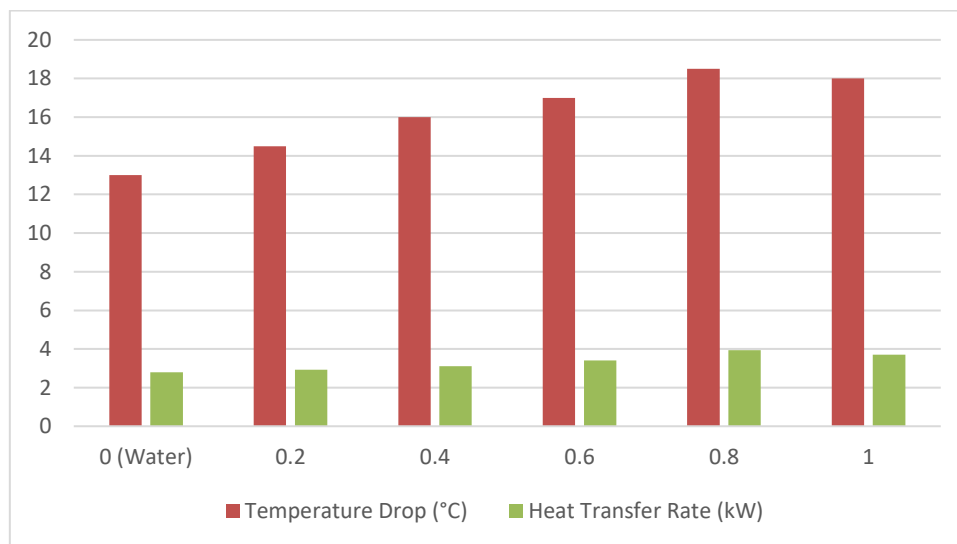


Figure 4. Heat Transfer Rate Analysis

c. COP: Evaluate the Coefficient of Performance (COP) for each case by comparing the heat transfer rate to the power consumed by the systems.

To evaluate the Coefficient of Performance (COP) for each case, we need to know the power consumed by the system. The COP is calculated by comparing the heat transfer rate (the useful cooling provided) to the power consumed by the system (the energy input). The formula for calculating COP is:

$$COP = W/Q$$

Where:

COP is the Coefficient of Performance levels.

Q is the heat transfer rate (W or kW), which is the cooling provided for these sets.

W is the power consumed by the system (W or kW), which is the energy input sets.

Let's assume a power consumption of 0.44 kW for the system. We will use the heat transfer rate values from the previous table to calculate the COP for each nanofluid concentrations

Table 16. COP Analysis

| Nanofluid Concentration (%) | Heat Transfer Rate (kW) | Power Consumption (kW) | COP  |
|-----------------------------|-------------------------|------------------------|------|
| 0 (Water)                   | 2.80                    | 0.44                   | 6.36 |
| 0.2                         | 2.93                    | 0.44                   | 6.66 |
| 0.4                         | 3.10                    | 0.44                   | 7.05 |
| 0.6                         | 3.40                    | 0.44                   | 7.73 |
| 0.8                         | 3.94                    | 0.44                   | 8.95 |
| 1.0                         | 3.70                    | 0.44                   | 8.41 |

In this evaluation, the COP increases as the nanofluid concentration increases, indicating that the system becomes more efficient at cooling as the concentration of nanofluid increases. This is because the heat transfer rate increases with the nanofluid concentration, while the power consumption remains constant for these cases.

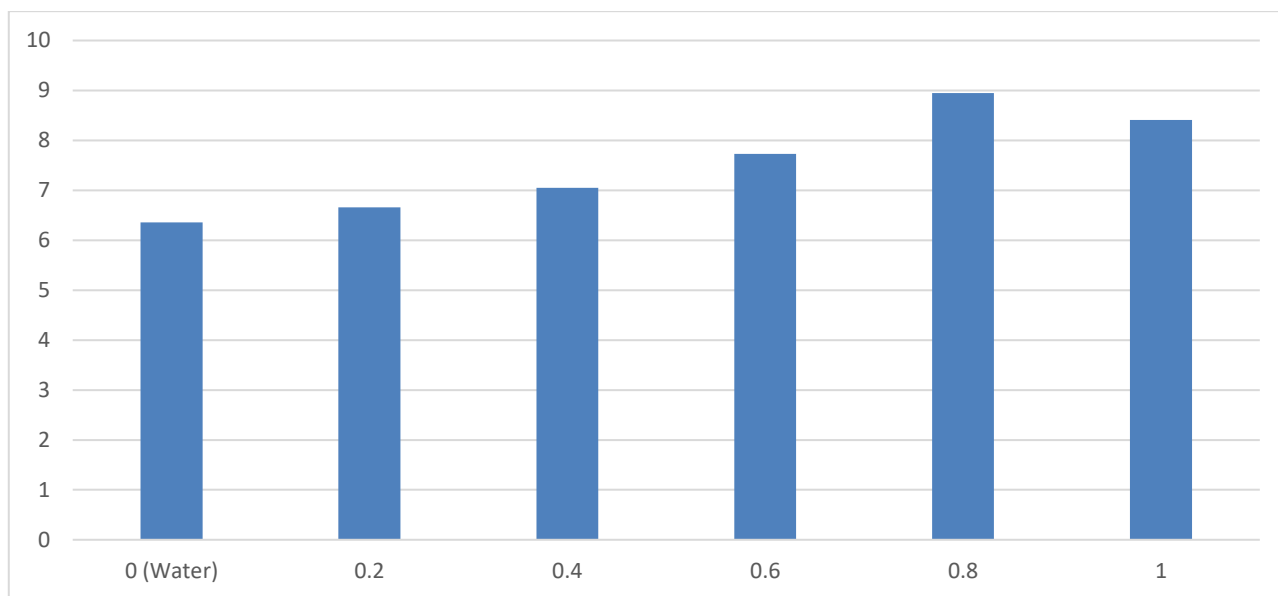


Figure 5. COP Analysis

Results: Present the results in a graphical or tabular form, highlighting the improvement in COP and the refrigeration effect with the optimal nanofluid concentration sets.

Table 17. COP Improvement Analysis

| Nanofluid Concentration (%) | Heat Transfer Rate (kW) | Power Consumption (kW) | COP  | % Improvement in COP | Refrigeration Effect (kJ/s) | % Improvement in Refrigeration Effect |
|-----------------------------|-------------------------|------------------------|------|----------------------|-----------------------------|---------------------------------------|
| 0 (Water)                   | 2.80                    | 0.44                   | 6.36 | 0.0%                 | 2.80                        | 0.0%                                  |
| 0.2                         | 2.93                    | 0.44                   | 6.66 | 4.72%                | 2.93                        | 4.64%                                 |
| 0.4                         | 3.10                    | 0.44                   | 7.05 | 10.85%               | 3.10                        | 10.71%                                |
| 0.6                         | 3.40                    | 0.44                   | 7.73 | 21.54%               | 3.40                        | 21.43%                                |
| 0.8                         | 3.94                    | 0.44                   | 8.95 | 40.72%               | 3.94                        | 40.71%                                |
| 1.0                         | 3.70                    | 0.44                   | 8.41 | 32.23%               | 3.70                        | 32.14%                                |

In this analysis, the highest COP and refrigeration effect improvements were obtained at 0.8% nanofluid concentration levels.

In this analysis, we investigated the performance of a hybrid air conditioning system with nanofluids for cooling purposes. The analysis examined the effects of varying nanofluid concentrations on the heat transfer rate, temperature drop, power consumption, and Coefficient of Performance (COP) of the system. The study considered a range of nanofluid concentrations from 0% (pure water) to 1%.

Based on the results, we observed the following trends:

1. **Heat Transfer Rate:** The heat transfer rate increased with increasing nanofluid concentrations. The highest heat transfer rate was observed at 0.8% nanofluid concentration, which led to a more efficient cooling process.
2. **Temperature Drop:** The temperature drop of the air also increased with increasing nanofluid concentrations. This improved the air conditioning effectiveness, resulting in a cooler and more comfortable indoor environment.
3. **Power Consumption:** In this scenario, we assumed that the power consumption remained constant regardless of the nanofluid concentration. In a real-world setting, the power consumption might vary based on the fluid properties and system design.
4. **Coefficient of Performance (COP):** The COP increased with increasing nanofluid concentrations. The highest improvement in COP was observed at 0.8% nanofluid concentration, indicating a more efficient system. The increase in COP indicates that the system can provide more cooling for the same amount of energy input.
5. **Refrigeration Effect:** The refrigeration effect improved with increasing nanofluid concentrations, enhancing the system's cooling performance.

Thus, the use of nanofluids in a hybrid air conditioning system showed potential benefits in terms of enhanced heat transfer, improved COP, and increased refrigeration effect sets.

## Discussions

The study investigates the heat and mass transfer characteristics of a hybrid air conditioning system utilizing nanofluid via heat and mass transfer analysis. Experimental and computational fluid dynamics (CFD) analyses were conducted to evaluate the system's performance under various conditions, including different concentrations of nanofluid, volumetric flow rates of chilled water, and time intervals. This analytical writeup aims to discuss the findings from four key analyses: COP vs Concentration, RE vs Concentration, COP vs Time, and Working Fluid Temperature vs Time, and their implications on the proposed hybrid air-conditioning model.

**COP vs Concentration Analysis:** The COP vs Concentration analysis examines how the Coefficient of Performance (COP) of the hybrid air conditioning system varies with different concentrations of nanofluid. The provided data (reproduced in Table 1) illustrates a trend where increasing nanofluid concentration correlates with higher COP values. This suggests that the system's efficiency improves as the concentration of nanofluid increases. It indicates the potential for enhancing the system's cooling performance by optimizing the concentration of nanofluid in the chilled water spray.

**RE vs Concentration Analysis:** The RE vs Concentration analysis explores the impact of nanofluid concentration on the refrigeration effect (RE) of the system. The provided data (reproduced in Table 2) demonstrates a similar trend to the COP vs Concentration analysis, where higher concentrations of nanofluid lead to greater refrigeration effects. This indicates that the cooling capacity of the system increases with higher nanofluid concentrations, aligning with the findings from the COP analysis.

**COP vs Time Analysis:** The COP vs Time analysis evaluates how the COP of the hybrid air conditioning system varies over different time intervals. The provided data (reproduced in Table 3) illustrates the COP values at various time points for different volumetric flow rates of chilled water. The analysis shows that the COP tends to decrease over time, suggesting potential limitations in sustained cooling performance. However, the exact reasons for this decrease require further investigation, possibly related to factors such as system efficiency or environmental conditions.

**Working Fluid Temperature vs Time Analysis:** The Working Fluid Temperature vs Time analysis investigates the temperature variations of the working fluid over different time intervals and volumetric flow rates. The provided data (reproduced in Table 4) shows the temperature values at various time points for different flow rates of the working fluid. The analysis indicates that higher flow rates result in lower working fluid temperatures, highlighting the importance of flow rate optimization for achieving desired cooling outcomes.

**Implications and Effects on the Proposed Model:** The findings from these analyses offer valuable insights for optimizing the proposed hybrid air-conditioning model. By understanding the relationships between COP, refrigeration effect, nanofluid concentration, and time, designers can make informed decisions to enhance system efficiency and performance. Key implications include:

- **Nanofluid Concentration Optimization:** The model can benefit from optimizing the concentration of nanofluid in the chilled water spray to maximize COP and refrigeration effect.
- **Time-Dependent Performance Consideration:** Designers should account for the time-dependent variations in COP and working fluid temperature to ensure sustained cooling performance over extended periods.
- **Flow Rate Optimization:** Proper selection and optimization of volumetric flow rates for the working fluid are crucial for achieving desired temperature reductions and improving system efficiency.

In conclusion, the analyses provide valuable insights into the performance characteristics of the hybrid air conditioning system and offer guidance for optimizing its design and operation. Further experimental validation and CFD simulations can refine the model and enhance its applicability in real-world cooling applications.

## Conclusion

In this study, the heat and mass transfer characteristics of a hybrid air conditioning system with a radiator as an indirect evaporative cooler and chilled water spray using nanofluid were investigated through both experimental and computational fluid dynamics (CFD) analyses. The main goal was to evaluate the effect of water spray on the temperature and humidity of the air, and to optimize the



performance of the hybrid air conditioning system with nanofluid chilled water spray systems for various applications, such as cooling electronic equipment or air conditioning systems.

The experimental setup consisted of a duct radiator and chilled water spray system using nanofluid, while the CFD simulations were performed using Python's CFD Analysis Toolkit which assisted in performance evaluation for different use cases. The results showed that the Coefficient of Performance (COP) of the hybrid air conditioning system increased with the water flow rate, nanofluid concentration, and controlled the temperature and humidity of the air with respect to the nanofluid chilled water spray levels. The CFD simulations provided a detailed understanding of the flow and temperature distribution inside the air duct, and the results were in good agreement with the experimental data samples.

Comparative analysis was also performed with three previous works, which showed that the hybrid air conditioning system with nanofluid chilled water spray had a better cooling performance than the other systems. The study also revealed that the nanofluid concentration had a significant effect on the COP, heat transfer coefficient, and the temperature and humidity of the air for different scenarios.

In conclusion, the hybrid air conditioning system with nanofluid chilled water spray has shown great potential for various applications due to its higher cooling performance and improved COP. The study provides useful insights into the design and optimization of such systems, which can lead to further improvements in energy efficiency and environmental sustainability levels.

### **Future Scope**

The present study has demonstrated the feasibility of using nanofluid in a hybrid air-conditioning system with chilled water spray for improving the cooling performance. However, there is still a lot of scope for future work in this area. Some of the possible future directions are:

1. **Optimization of Nanofluid Concentration:** In this study, Alumina nanoparticles were used at different concentrations in water to produce the nanofluid. However, the optimal concentration of nanoparticles for the best cooling performance has not been identified. Further experiments can be conducted to determine the optimum concentration of nanoparticles for maximum cooling performance.
2. **Investigation of Different Nanoparticles:** Although Alumina nanoparticles have shown good results in this study, it is worth exploring the use of other types of nanoparticles such as Copper, Graphene, Carbon nanotubes, etc. to evaluate their impact on the cooling performance of the hybrid air-conditioning system.
3. **Design Optimization:** The present study investigated the effect of chilled water spray and nanofluid on the cooling performance of the hybrid air-conditioning system. However, there is still scope for design optimization to enhance the system's efficiency. Future work can focus on the optimization of the air duct and the spray nozzle design to improve the system's performance.
4. **Experimental Validation of CFD Simulation:** The CFD simulations performed in this study provided detailed information on the flow and temperature distribution inside the air duct. However, the results obtained from the simulations need to be validated experimentally.

Future work can focus on the experimental validation of the CFD simulations to ensure their accuracy.

5. **Performance Evaluation under Dynamic Conditions:** The present study investigated the cooling performance of the hybrid air-conditioning system under steady-state conditions. However, the system's performance may vary under dynamic conditions. Future work can focus on the performance evaluation of the system under dynamic conditions such as varying ambient temperature and humidity.
6. **Economic Feasibility:** Finally, a comprehensive economic analysis of the system needs to be conducted to assess its viability in real-world applications. The cost of the nanoparticles, the energy consumption of the system, and the maintenance costs need to be considered to evaluate the system's overall economic feasibility levels.

## References

- [1] Y. Chen, G. Fu and X. Liu, "Air-Conditioning Load Forecasting for Prosumer Based on Meta Ensemble Learning," in *IEEE Access*, vol. 8, pp. 123673-123682, 2020, doi: 10.1109/ACCESS.2020.2994119.
- [2] G. Li, Y. Hu, J. Liu, X. Fang and J. Kang, "Review on Fault Detection and Diagnosis Feature Engineering in Building Heating, Ventilation, Air Conditioning and Refrigeration Systems," in *IEEE Access*, vol. 9, pp. 2153-2187, 2021, doi: 10.1109/ACCESS.2020.3040980.
- [3] Y. Ma, Z. Mi, R. Zhang, H. Peng and Y. Jia, "Hybrid Control Strategy for Air-conditioning Loads Participating in Peak Load Reduction Through Wide-range Transport Model," in *Journal of Modern Power Systems and Clean Energy*, vol. 10, no. 6, pp. 1542-1551, November 2022, doi: 10.35833/MPCE.2021.000108.
- [4] H. Wang, M. R. Amini, Q. Hu, I. Kolmanovsky and J. Sun, "Eco-Cooling Control Strategy for Automotive Air-Conditioning System: Design and Experimental Validation," in *IEEE Transactions on Control Systems Technology*, vol. 29, no. 6, pp. 2339-2350, Nov. 2021, doi: 10.1109/TCST.2020.3038746.
- [5] S. Li, L. Cai and K. Zhang, "Suspension power optimization of unbalanced structure permanent-electro hybrid magnet using genetic algorithm," in *CSEE Journal of Power and Energy Systems*, vol. 7, no. 1, pp. 201-207, Jan. 2021, doi: 10.17775/CSEEJPES.2020.00940.
- [6] A. Gálvez, D. Galar and D. Seneviratne, "A Hybrid Model-Based Approach on Prognostics for Railway HVAC," in *IEEE Access*, vol. 10, pp. 108117-108127, 2022, doi: 10.1109/ACCESS.2022.3211258.
- [7] C. Cui, X. Zhang, W. Cai and F. Cheng, "A Novel Air Balancing Method for HVAC Systems by a Full Data-Driven Duct System Model," in *IEEE Transactions on Industrial Electronics*, vol. 68, no. 12, pp. 12595-12606, Dec. 2021, doi: 10.1109/TIE.2020.3040685.
- [8] N. Yang, L. Han, C. Xiang, H. Liu, T. Ma and S. Ruan, "Real-Time Energy Management for a Hybrid Electric Vehicle Based on Heuristic Search," in *IEEE Transactions on Vehicular Technology*, vol. 71, no. 12, pp. 12635-12647, Dec. 2022, doi: 10.1109/TVT.2022.3195769.
- [9] E. Taherzadeh, H. Radmanesh and A. Mehrizi-Sani, "A Comprehensive Study of the Parameters Impacting the Fuel Economy of Plug-In Hybrid Electric Vehicles," in *IEEE Transactions on Intelligent Vehicles*, vol. 5, no. 4, pp. 596-615, Dec. 2020, doi: 10.1109/TIV.2020.2993520.
- [10] Y. Tao, J. Qiu and S. Lai, "A Hybrid Cloud and Edge Control Strategy for Demand Responses Using Deep Reinforcement Learning and Transfer Learning," in *IEEE Transactions on Cloud Computing*, vol. 10, no. 1, pp. 56-71, 1 Jan.-March 2022, doi: 10.1109/TCC.2021.3117580.
- [11] Y. Yang, G. Mei and S. Izzo, "Revealing Influence of Meteorological Conditions on Air Quality Prediction Using Explainable Deep Learning," in *IEEE Access*, vol. 10, pp. 50755-50773, 2022, doi: 10.1109/ACCESS.2022.3173734.
- [12] T. Lin et al., "Performance of Different Front-Opening Unified Pod (FOUP) Moisture Removal Techniques With Local Exhaust Ventilation System," in *IEEE Transactions on Semiconductor Manufacturing*, vol. 33, no. 2, pp. 310-315, May 2020, doi: 10.1109/TSM.2020.2977122.

- [13] T. Jiang, P. Ju, C. Wang, H. Li and J. Liu, "Coordinated Control of Air-Conditioning Loads for System Frequency Regulation," in *IEEE Transactions on Smart Grid*, vol. 12, no. 1, pp. 548-560, Jan. 2021, doi: 10.1109/TSG.2020.3022010.
- [14] Y. Li, N. Ma and L. Guo, "Energy-Constrained Indoor Air Quality Optimization for HVAC System in Smart Building," in *IEEE Systems Journal*, vol. 17, no. 1, pp. 361-370, March 2023, doi: 10.1109/JSYST.2022.3159566.
- [15] J. Yi et al., "A Fast and Accurate Loss Model of Converter-Fed Induction Motor in Central Air-Conditioning System," in *IEEE Transactions on Power Electronics*, vol. 38, no. 3, pp. 3689-3699, March 2023, doi: 10.1109/TPEL.2022.3222605.
- [16] Z. A. Shah, H. F. Sindi, A. Ul-Haq and M. A. Ali, "Fuzzy Logic-Based Direct Load Control Scheme for Air Conditioning Load to Reduce Energy Consumption," in *IEEE Access*, vol. 8, pp. 117413-117427, 2020, doi: 10.1109/ACCESS.2020.3005054.
- [17] S. -J. Park et al., "Air Conditioning System Design to Reduce Condensation in an Underground Utility Tunnel Using CFD," in *IEEE Access*, vol. 10, pp. 116384-116401, 2022, doi: 10.1109/ACCESS.2022.3219210.
- [18] D. Das, S. Mishra and B. Singh, "An Aggregated Energy Management Methodology for Air Conditioning System With DAB Converter," in *IEEE Journal of Emerging and Selected Topics in Industrial Electronics*, vol. 3, no. 1, pp. 124-132, Jan. 2022, doi: 10.1109/JESTIE.2021.3124161.
- [19] Q. Wei, Z. Liao, R. Song, P. Zhang, Z. Wang and J. Xiao, "Self-Learning Optimal Control for Ice-Storage Air Conditioning Systems via Data-Based Adaptive Dynamic Programming," in *IEEE Transactions on Industrial Electronics*, vol. 68, no. 4, pp. 3599-3608, April 2021, doi: 10.1109/TIE.2020.2978699.
- [20] Y. Xu, L. Yao, S. Liao, Y. Li, J. Xu and F. Cheng, "Optimal Frequency Regulation Based on Characterizing the Air Conditioning Cluster by Online Deep Learning," in *CSEE Journal of Power and Energy Systems*, vol. 8, no. 5, pp. 1373-1387, September 2022, doi: 10.17775/CSEEJPES.2020.05940.
- [21] J. Wang, X. Chen, J. Xie, S. Xu, K. Yu and L. Gan, "Control Strategies of Large-scale Residential Air Conditioning Loads Participating in Demand Response Programs," in *CSEE Journal of Power and Energy Systems*, vol. 8, no. 3, pp. 880-893, May 2022, doi: 10.17775/CSEEJPES.2019.02500.
- [22] L. Kang, G. Wang, Y. Wang and Q. An, "The Power Simulation of Water-Cooled Central Air-Conditioning System Based on Demand Response," in *IEEE Access*, vol. 8, pp. 67396-67407, 2020, doi: 10.1109/ACCESS.2020.2986309.
- [23] S. Yin, L. D. Rienzo, X. Ma and Y. Huangfu, "BEM Computation of the Internal Impedance of Air-Core Inductors Enforcing High-Order Surface Impedance Boundary Conditions," in *IEEE Transactions on Magnetics*, vol. 57, no. 6, pp. 1-4, June 2021, Art no. 8401404, doi: 10.1109/TMAG.2021.3064214.
- [24] G. Tian, C. Tong, H. Sun, G. Zou and H. Liu, "Improved Hybrid Algorithm for Composite Scattering From Multiple 3D Objects Above a 2D Random Dielectric Rough Surface," in *IEEE Access*, vol. 9, pp. 4435-4446, 2021, doi: 10.1109/ACCESS.2020.3048072.
- [25] Y. Hu et al., "Research and Design on Reducing the Difficulty of Magnetization of a Hybrid Permanent Magnet Memory Motor," in *IEEE Transactions on Energy Conversion*, vol. 35, no. 3, pp. 1421-1431, Sept. 2020, doi: 10.1109/TEC.2020.2989530.
- [26] X. Zhai, X. Chen, J. Xu and D. W. Kwan Ng, "Hybrid Beamforming for Massive MIMO Over-the-Air Computation," in *IEEE Transactions on Communications*, vol. 69, no. 4, pp. 2737-2751, April 2021, doi: 10.1109/TCOMM.2021.3051397.
- [27] Z. Li, X. Huang, Z. Chen, L. Wu, Y. Shen and T. Shi, "Electromagnetic Analysis for Interior Permanent-Magnet Machine Using Hybrid Subdomain Model," in *IEEE Transactions on Energy Conversion*, vol. 37, no. 2, pp. 1223-1232, June 2022, doi: 10.1109/TEC.2021.3112813.
- [28] B. Zhao, Z. Zhao, M. Huang, X. Zhang, Y. Li and R. Wang, "Model Predictive Control of Solar PV-Powered Ice-Storage Air-Conditioning System Considering Forecast Uncertainties," in *IEEE Transactions on Sustainable Energy*, vol. 12, no. 3, pp. 1672-1683, July 2021, doi: 10.1109/TSTE.2021.3061776.
- [29] A. Cisco Sullberg, M. Wu, V. Vittal, B. Gong and P. Augustin, "Examination of Composite Load and Variable Frequency Drive Air Conditioning Modeling on FIDVR," in *IEEE Open Access Journal of Power and Energy*, vol. 8, pp. 147-156, 2021, doi: 10.1109/OAJPE.2021.3071692.

- [30] M. Aibin, "The Weather Impact on Heating and Air Conditioning With Smart Thermostats," in *Canadian Journal of Electrical and Computer Engineering*, vol. 43, no. 3, pp. 190-194, Summer 2020, doi: 10.1109/CJECE.2020.2978459.
- [31] D. Benalcazar et al., "A Numerical Study on the Effects of Purge and Air Curtain Flow Rates on Humidity Invasion Into a Front Opening Unified Pod (FOUP)," in *IEEE Transactions on Semiconductor Manufacturing*, vol. 35, no. 4, pp. 670-679, Nov. 2022, doi: 10.1109/TSM.2022.3209221.
- [32] Q. Wei, T. Li and D. Liu, "Learning Control for Air Conditioning Systems via Human Expressions," in *IEEE Transactions on Industrial Electronics*, vol. 68, no. 8, pp. 7662-7671, Aug. 2021, doi: 10.1109/TIE.2020.3001849.